Phase retrieval in x-ray imaging based on using structured illumination

Y. J. Liu,[1,3] B. Chen,[2] E. R. Li,[1] J. Y. Wang,[1] A. Marcelli,[4] S. W. Wilkins,[5] H. Ming,[3] Y. C. Tian,[6] K. A. Nugent,[2,*] P. P. Zhu,[1,†] and Z. Y. Wu[1,6,7,‡]

[1]*Institute of High Energy Physics, Chinese Academy of Science, Beijing 100049, China*
[2]*School of Physics, The University of Melbourne, Victoria 3010, Australia*
[3]*Department of Physics, University of Science and Technology of China, Hefei 230026, China*
[4]*INFN-Laboratori Nazionali di Frascati, Via E. Fermi 40, I-00044 Frascati, Rome 00146, Italy*
[5]*Commonwealth Scientific and Industrial Research Organisation, PB 33, Clayton South, Victoria 3169, Australia*
[6]*National Synchrotron Radiation Laboratory, University of Science and Technology of China, Hefei 230026, China*
[7]*Theoretical Physics Center for Science Facilities, Chinese Academy of Sciences, Beijing 100049, China*

(Received 12 November 2007; published 11 August 2008)

A different x-ray phase contrast imaging technique based on the combination of structured illumination and an optimized hybrid input-output algorithm for phase and amplitude retrieval is presented and discussed. Based on a modified and flexible experimental setup, compared to standard propagation-based x-ray imaging setups, the method we propose here represents a real advance in the phase-contrast imaging technique relating to the determination of the phase and amplitude distribution. Moreover, in coherent diffractive imaging applications, the proposed technique may yield high spatial resolution with currently available imaging detectors.

DOI: 10.1103/PhysRevA.78.023817 PACS number(s): 42.30.Rx, 87.59.−e, 87.64.Bx

I. INTRODUCTION

Over the past few decades, x-ray phase-contrast imaging (XPCI) has become a powerful tool for structural investigations [1–5]. A wide range of applications spanning industrial research to biomedical investigations has benefited from the availability of these techniques. In this regard, the determination of the phase is highly desirable, since it relates to a fundamental property of the material, namely, the projected electron density. To fulfill this task of phase determination from the measured intensity distribution, several methods have been proposed. Among them, the in-line or propagation-based (PB-PCI) x-ray phase-contrast imaging techniques are the simplest and most widely used among the available experimental methods. The possibility to extract a quantitative phase map from propagation-based XPCI was first achieved by Nugent *et al.* [6] in a direct way applying the transport of intensity equation (TIE) to perform phase retrieval [7–9] based on using monochromatic data from a synchrotron source. Separately, Wilkins *et al.* [4] showed that polychromatic x rays could be used for x-ray in-line imaging and, working within the same framework of the TIE, Gureyev and Wilkins also described methods for phase retrieval using polychromatic data [10–12]. The phase retrieval problem is a difficult task to manage in practice because the longitudinal derivative of the intensity, $\partial I/\partial z$, of the propagating x-ray beam, which is involved in the TIE equation, requires the accurate collection of images at least at two different distances from the sample [13] or at two different energies [10–12]. Meanwhile, the development of indirect methods of phase recovery has become an active field of investigation. For the near-field diffraction case, multi-plane image intensity measurements, recorded over planes at a series of distances along the optical axis, have been used to produce quantitative phase recovery [14,15]. Another method to collect adequate data (three or more diffraction patterns in a given viewing angle) for quantitative phase retrieval within the Fresnel region was proposed by Zhang *et al.* [16], in which different wave front modulation is performed for every exposure. For the far-field diffraction case [17–28] (better known as coherent diffractive imaging techniques), the oversampling approach is used together with the hybrid input-output (HIO) algorithm and a support constraint, to yield successful phase recovery in many cases [29–33].

In this contribution, we discuss the possibility of performing an XPCI experiment for the purpose of providing an improved method for phase and amplitude retrieval via the use of a structured incident x-ray beam. This structure in the beam can be introduced either by inserting a reference phase mask along the optical system or by illuminating the sample with two interfering coherent beams. Both approaches are equivalent, as confirmed by numerical simulations. With the use of the structured illumination for the imaging system, we succeed in extracting the quantitative phase and amplitude distribution from two diffraction patterns taken in opposite viewing angles of the sample. As a result, the only mechanical movement of the whole imaging system is the rotation of the sample in a CT scan, which is indispensable for three-dimensional (3D) reconstruction.

II. STRUCTURED ILLUMINATION BASED XPCI SCHEME AND ALGORITHM

The experimental setup for x-ray in-line imaging of a complex object using structured illumination is illustrated in Fig. 1. In this scheme, a reference mask of known structure is placed upstream of the object to be investigated and the intensity distribution is recorded within the Fresnel diffraction

*k.nugent@physics.unimelb.edu.au
†zhupp@ihep.ac.cn
‡wuzy@ihep.ac.cn

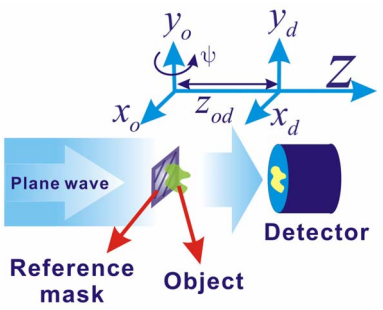

FIG. 1. (Color online) Schematic layout of the experimental setup for x-ray in-line imaging experiments with structured illumination produced by a reference mask set along the optical path upstream of the sample.

regime. The method has conceptual links with the method of Fresnel coherent diffractive imaging (FCDI) [24] in that it imposes a structure on the incident field, either in the form of a phase curvature (as in FCDI, see Ref. [24]) or other structured illumination as outlined here.

In order to collect the data necessary to solve for the phase distribution, rather than moving the detector along the optical axis as discussed earlier, we instead collect data with a combination of object and mask configurations, i.e., collecting data in opposite viewing angles of the sample, as illustrated in Fig. 2.

The proposed experiment has been simulated using the Fresnel diffraction formula [33], which describes the wave propagation. Starting from an initial estimation of the complex refractive index distribution of the sample, we choose

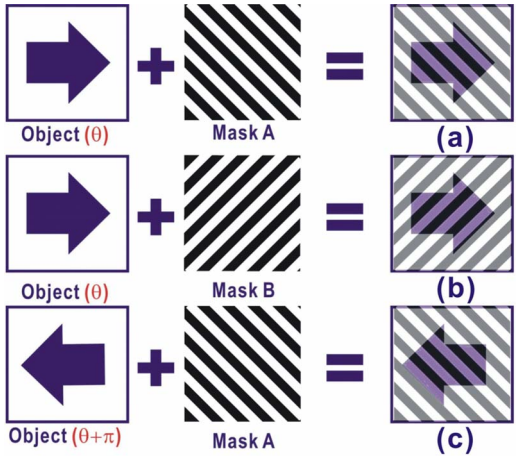

FIG. 2. (Color online) Schemes showing how an experimental layout with a fixed reference mask associated with a sample that is free to rotate over a wide angular range permits an equivalent combined object data set to that obtained using a layout with two different reference masks. Panel (a) shows the sample set at the angle of view θ of the object with respect to the reference mask A. Panel (b) refers to the same sample at the same viewing angle θ, but after a rotation of the mask around the vertical axis by 180 degree. Panel (c) shows the same sample as seen from the opposite angle $\theta+\pi$ with respect to the mask orientation in panel (a). This latter geometry is equivalent to that of the panel (b) via a simple coordinate transformation.

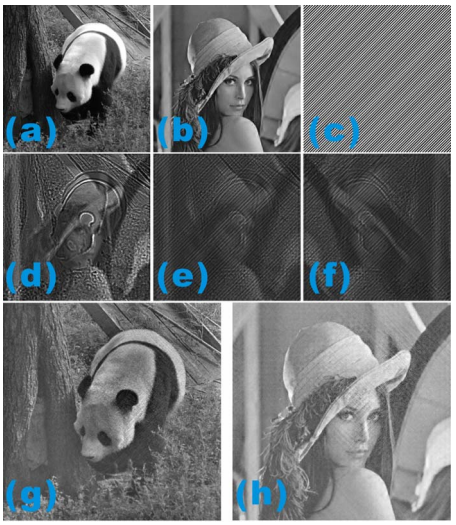

FIG. 3. (Color online) Comparison among simulations of the modified HIO phase retrieval algorithm, as discussed in the text. The distributions of the real and the imaginary parts of the complex object involved in our simulation are presented in panels (a) and (b), respectively; panel (c) denotes the phase mask; the simulated Fresnel diffraction pattern both with and without the mask on is demonstrated in panels (d) and (e); while panel (f) is the recorded image with mask in place but in the opposite viewing angle of the sample; the recovered argument distribution and the amplitude distribution of the wave field over the exit plane of the sample are shown in panels (g) and (H).

the HIO algorithm, which is optimized for the proposed scheme, to return an improved image at each cycle. To investigate the proposed method, we simulated different x-ray Fresnel near-field imaging experiments where the parameters of the optical system have been set according to the effective layout, e.g., the sample size was set to 1.4 mm$\times$1.4 mm with a thickness of 100 μm, the distance from sample to detector was set to 80 cm, and the resolution of the detector was set to 2 μm. The reference mask involved (i.e., a π phase grating with a period of 18 μm, see Fig. 3(c), in order to obtain information associated with the interference pattern, should be able to cover the investigated field of view and is set to be of the same size as the sample in our simulation. According to the restriction implied by Eq. (1), the detector is placed far enough to ensure that the diffraction patterns at the detector plane with respect to the angles of view θ and $\theta+\pi$ of the sample are independent from each other due to the asymmetry of the reference mask,

$$z_{od} \geqslant \frac{T^2}{4\lambda}. \tag{1}$$

In Eq. (1), T is the period of the reference mask while λ is the wavelength of the incident x-ray beam.

Considering that we work with a plane monochromatic x-ray beam at an energy of 10 keV, a complex object is employed for our numerical simulations, with the real part of the refractive index decrement ranging from 0 to 10^{-6} while the imaginary part ranges from 0 to 10^{-7}, as illustrated in Figs. 3(a) and 3(b), respectively. Fresnel diffraction calcula-

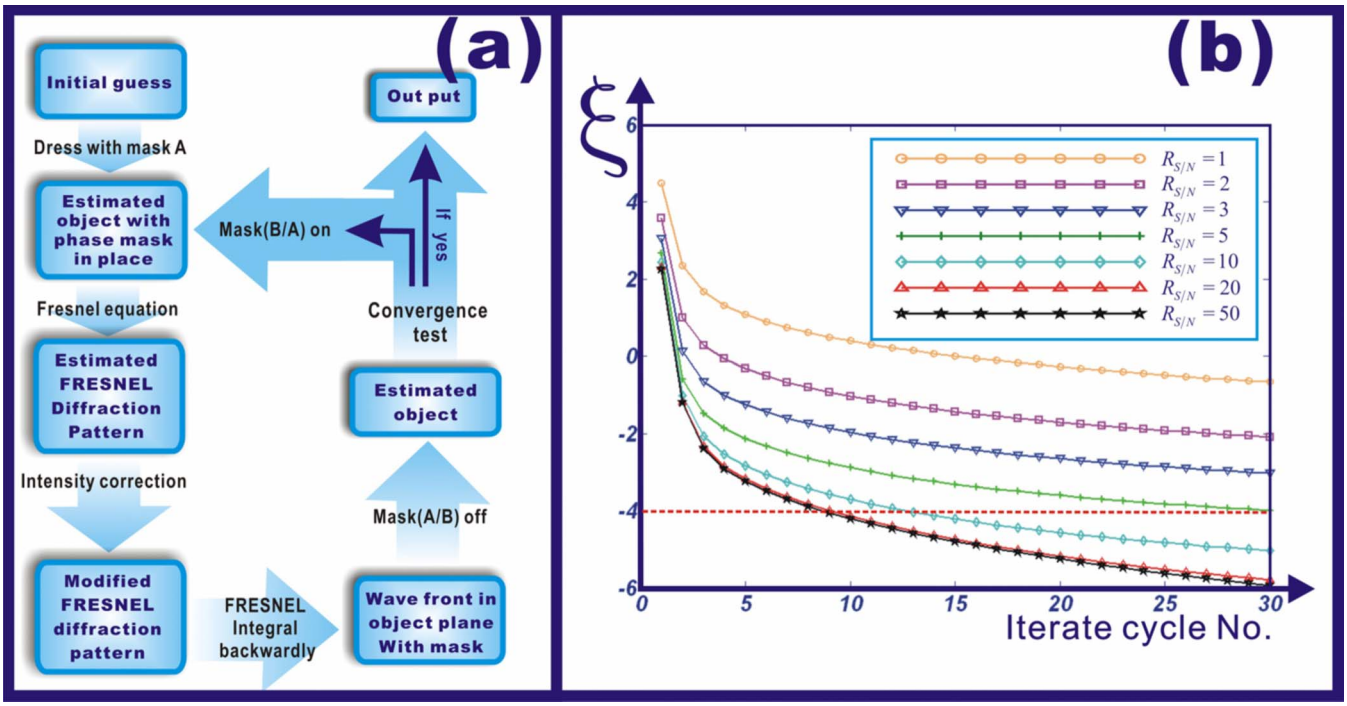

FIG. 4. (Color online) The flow chart of the modified HIO algorithm is presented in panel (a), while the behavior of ξ, the representative fitting parameter for the HIO algorithm, versus the iteration cycle with respect to different signal-to-noise ratios is shown in panel (b).

tions of images were performed both with and without the reference mask [Fig. 3(c)]. The corresponding Fresnel diffraction patterns at the detector plane are shown in Fig. 3(d) without mask), 3(e) (with mask), and 3(f) (in the opposite view angle and with mask), respectively. Assuming no support but a knowledge of the mask and refining on the two Fresnel diffraction patterns recorded with the phase mask in place (both Figs. 3(e) and 3(f)], the iterative phase retrieval algorithm yielded, successfully, both the phase distribution [Fig. 3(g)] and the amplitude distribution [Fig. 3(h)] of the wavefield over the exit plane of the sample.

To better understand and evaluate the performance of the algorithm, the flow chart of the modified HIO algorithm, which is optimized for our case, is demonstrated in Fig. 4(a). As demonstrated in Fig. 4(a), the algorithm can be summarized as follows:

$$U_{\text{obj}}^{i+1} = A_{\text{switch}}\left(\frac{i\mathcal{F}\{I_{\text{correction}}[\mathcal{F}(U_{\text{obj}}^{i}U_{\text{mask}})]\}}{U_{\text{mask}}}\right), \tag{2}$$

where U_{obj}^{i} denotes the estimated wave field after i iterations; U_{mask} denotes the effect induced by the phase mask; $\mathcal{F}$ and $i\mathcal{F}$, respectively, stand for the numerical calculation of the Fresnel diffraction forward and backward; $I_{\text{correction}}$ denotes a function that modifies the estimated intensity distribution of the wave field over the detector plane according to the one measured experimentally; and A_{switch} denotes the switch of the viewing angle [see Figs. 3(e) and 3(f)].

We also introduced the goodness-of-fit parameter, ξ, which is defined as follows:

$$\xi = \log\left\{\frac{\int\int_{\Sigma}\left(\frac{I_{(x,y)}^{\text{estimated}} - I_{(x,y)}^{\text{exp}}}{I_{\text{mean}}^{\text{exp}}}\right)^{2} dxdy}{\int\int_{\Sigma} dxdy}\right\}, \tag{3}$$

in which (x,y) is the coordinate system associated with the detector plane while I is the intensity distribution over the detector plane. Actually ξ is also a suitable parameter to evaluate the difference between the estimated intensity distribution and the experimental value. In Fig. 4(b), we show the exponential-like convergent behavior of the algorithm versus the iteration cycle with respect to different signal-to-noise ratios. For a typical value of the signal-to-noise ratio (R_{SN}=5 on both the incident wave field and the image recording system), the proposed algorithm reaches convergence ($\xi \leqslant -4$) within 30 iterations.

The results obtained are very encouraging. However, there are technical difficulties for fabricating masks with the required structure [34] to allow coherent diffractive imaging at very high spatial resolution. Therefore, we also performed simulations in which a structured illumination is obtained as a coherent interference pattern, as shown in Fig. 5(a). In the following discussion, we limited our considerations to the case of a pure phase object [see Fig. 3(a)] for the sake of simplicity. The amplitude and the argument distributions for the interference pattern over the plane upstream of the sample are outlined in Figs. 5(b) and 5(c), respectively, while the recovered phase map in this case is presented in Fig. 5(d).

III. DISCUSSION AND CONCLUSION

The simulations presented in this contribution demonstrate that structured illumination produced by a reference

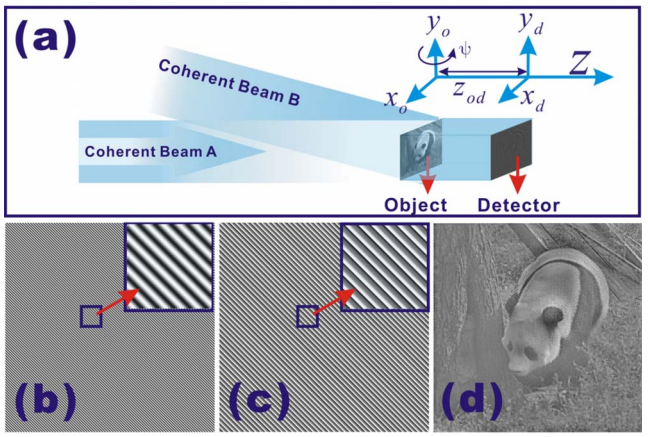

FIG. 5. (Color online) Structured illumination obtained as an interference pattern. A schematic layout of the experimental setup is shown in panel (a). The amplitude and the argument distributions of the interference pattern illuminating the sample are showed in panels (b) and (c), respectively. The recovered phase map is shown in panel (d).

mask placed along the optical axis combined with an x-ray Fresnel diffraction imaging and a modified HIO algorithm may significantly improve the ability to carry out phase retrieval in propagation-based x-ray in-line imaging. Moreover, when compared to the multiple-distance-based phase retrieval methods employed in the propagation-based x-ray imaging, the proposed approach would appear to allow for the possibility of working with a more convenient experimental layout and is also characterized by a simple phase retrieval procedure, which we have found is not very sensitive to the noise.

Finally, we investigated also a layout in which the structured illumination is achieved as a coherent interference pattern. Results show that, in principle, with this technique a successful phase recovery may also be obtained. In fact, the illumination of a sample with an asymmetric interference pattern is equivalent to the use of a physical mask. Moreover, a structured illumination obtained via a coherent interference pattern offers effective advantages and the possibility to be applied to the coherent diffractive imaging case.

A wide range of x-ray PCI techniques may benefit from the adoption of the proposed schemes, including the propagation-based x-ray imaging and also coherent diffractive imaging techniques. In fact, considering the traditional algorithms used for phase retrieval in propagation-based PCI (e.g., solving of the TIE) and in CDI (oversampling-based HIO), our method based on a modified HIO algorithm is versatile and allows for a more convenient experimental setup, optimizing also the use of a given detector, i.e., it is anticipated that the structured-illumination-based HIO algorithm for phase and amplitude retrieval in CDI applications would make better use of the available detector and may lead to better resolution, since the routinely used oversampling approach is no longer a necessary data process procedure in the proposed scheme.

In conclusion, due both to the use of structured illumination and to the performance of the modified HIO algorithm, the proposed method may be used to retrieve phase information in a straightforward way for a wide variety of cases.

ACKNOWLEDGMENTS

This work was partly supported by the National Outstanding Youth Fund (Project No. 10125523 to Z.W.); the Key Important Project of the National Natural Science Foundation of China (Grants No. 10490194 and No. 10734070); the National Natural Science Foundation of China (Grants No. 60477006, No. 10504033, and No. 10774144); the Knowledge Innovation Program of the Chinese Academy of Sciences (Grants No. KJCX2-SW-N11 and No. KJCX2-SW-H12-02); and by the National Center for Nanoscience and Technology of China. The support of the Australian Research Council is also acknowledged through the ARC Center of Excellence for Coherence X-ray Science.

[1] U. Bonse and M. Hart, Appl. Phys. Lett. **6**, 155 (1965).
[2] E. Forster *et al.*, Krist. Tech. **15**, 937 (1980).
[3] A. Sinigirev *et al.*, Rev. Sci. Instrum. **66**, 5486 (1995).
[4] S. W. Wilkins *et al.*, Nature **384**, 335 (1996).
[5] F. Pfeiffer *et al.*, Nat. Phys. **2**, 258 (2006).
[6] K. A. Nugent, Phys. Rev. Lett. **68**, 2261 (1992).
[7] K. A. Nugent, T. E. Gureyev, D. F. Cookson, D. Paganin, and Z. Barnea, Phys. Rev. Lett. **77**, 2961 (1996).
[8] D. Paganin and K. A. Nugent, Phys. Rev. Lett. **80**, 2586 (1998).
[9] P. J. McMahon *et al.*, Appl. Phys. Lett. **83**, 1480 (2003).
[10] T. E. Gureyev and S. W. Wilkins, Opt. Commun. **147**, 229 (1998).
[11] T. E. Gureyev, S. Mayo, S. W. Wilkins, D. Paganin, and A. W. Stevenson, Phys. Rev. Lett. **86**, 5827 (2001).
[12] T. E. Gureyev, D. M. Paganin, A. W. Stevenson, S. C. Mayo, and S. W. Wilkins, Phys. Rev. Lett. **93**, 068103 (2004).
[13] K. A. Nugent, J. Opt. Soc. Am. A **24**, 536 (2007).
[14] P. Cloetens *et al.*, J. Phys. D **29**, 133 (1996).
[15] L. J. Allen and M. P. Oxley, Opt. Commun. **199**, 65 (2001).
[16] F. Zhang, G. Pedrini, and W. Osten, Phys. Rev. A **75**, 043805 (2007).
[17] J. Miao *et al.*, Nature (London) **400**, 342 (1999).
[18] J. Miao, T. Ishikawa, B. Johnson, E. H. Anderson, B. Lai, and K. O. Hodgson, Phys. Rev. Lett. **89**, 088303 (2002).
[19] G. J. Williams, M. A. Pfeifer, I. A. Vartanyants, and I. K. Robinson, Phys. Rev. Lett. **90**, 175501 (2003).
[20] M. A. Pfeifer *et al.*, Nature (London) **442**, 63 (2006).
[21] H. N. Chapman *et al.*, Nat. Phys. **2**, 839 (2006).
[22] K. J. Gaffney and H. N. Chapman, Science **316**, 1444 (2007).
[23] H. M. Quiney *et al.*, Opt. Lett. **30**, 1638 (2005).
[24] X. Xiao and Q. Shen, Phys. Rev. B **72**, 033103 (2005).
[25] G. J. Williams, H. M. Quiney, B. B. Dhal, C. Q. Tran, K. A. Nugent, A. G. Peele, D. Paterson, and M. D. deJonge, Phys.

Rev. Lett. **97**, 025506 (2006).
[26] H. M. Quiney *et al.*, Nat. Phys. **2**, 101 (2006).
[27] H. M. L. Faulkner and J. M. Rodenburg, Phys. Rev. Lett. **93**, 023903 (2004).
[28] J. M. Rodenburg, A. C. Hurst, A. G. Cullis, B. R. Dobson, F. Pfeiffer, O. Bunk, C. David, K. Jefimovs, and I. Johnson, Phys. Rev. Lett. **98**, 034801 (2007).
[29] R. W. Gerchberg and W. O. Saxton, Optik (Stuttgart) **35**, 237 (1972).
[30] J. R. Fienup, Appl. Opt. **21**, 2758 (1982).
[31] V. Elser, J. Opt. Soc. Am. A **20**, 40 (2003).
[32] H. H. Bauschke *et al.*, J. Opt. Soc. Am. A **20**, 1025 (2003).
[33] M. Born and E. Wolf, *Principles of Optics*, 7th ed. (Cambridge University Press, Cambridge, 1999).
[34] W. Yun *et al.*, Rev. Sci. Instrum. **70**, 2238 (1999).